

1

[ATLAS Semivisible Jets]

2

[Elena Laura Busch]

3

Submitted in partial fulfillment of the
requirements for the degree of
Doctor of Philosophy
under the Executive Committee
of the Graduate School of Arts and Sciences

4

5

6

7

8

COLUMBIA UNIVERSITY

9

2024

10

© 2024

11

[Elena Laura Busch]

12

All Rights Reserved

13

Abstract

14

[ATLAS Semivisible Jets]

15

[Elena Laura Busch]

16

Abstract of dissertation (place-holder).

Table of Contents

18	Acknowledgments	v
19	Dedication	vi
20	Introduction or Preface	1
21	Chapter 1: The Standard Model	2
22	Chapter 2: The Large Hadron Collider	4
23	2.1 LHC Timeline	4
24	2.2 Accelerator Physics	5
25	2.2.1 The Journey of a Proton	5
26	2.2.2 Magnets	7
27	2.3 Luminosity	8
28	Chapter 3: The ATLAS Detector	10
29	3.1 Coordinate System and Geometry	10
30	3.2 Inner Detector	12
31	3.2.1 Pixel Detector	12
32	3.2.2 Semiconductor Tracker	13
33	3.2.3 Transition Radiation Tracker	13

34	3.3 Calorimeters	13
35	3.3.1 Liquid Argon Calorimeter	14
36	3.3.2 Tile Calorimeter	18
37	Conclusion or Epilogue	20
38	References	24
39	Appendix A: Experimental Equipment	26
40	Appendix B: Data Processing	27

List of Figures

42	2.1	Timeline of LHC activities [9]	5
43	2.2	The LHC accelerator complex at CERN [11]	6
44	2.3	The octants of the LHC and location of various beam activities [10]	8
45	3.1	ATLAS coordinate system and geometry	12
46	3.2	ATLAS calorimetery system [13]	14
47	3.3	Diagram of a segment of the EMB, demonstrating the accordion plate arrangement [14]	16
49	3.4	A LAr pulse as produced in the detector (triangle) and after shaping (curve) [14]	17
50	3.5	Readout gap structure in HEC [14]	17
51	3.6	TileCal wedge module [17]	19

List of Tables

53

Acknowledgements

54 Insert your acknowledgements text here. This page is optional, you may delete it if not

55 needed.

56

Dedication

57

Dedicated to my friends and family

58

Introduction or Preface

59 Insert your preface text here if applicable. This page is optional, you may delete it if not
60 needed. If you delete this page make sure to move page counter comment in thesis.tex to correct
61 location.

62

63

Chapter 1: The Standard Model

64 Four fundamental forces

65 The Standard Model is a universally accepted framework which explains most of the interactions
66 of fundamental particles. The SM is a renormalizable quantum field theory that obeys the
67 local symmetry G_{SM} :

$$G_{SM} = SU(3)_C \times SU(2)_L \times U(1)_Y \quad (1.1)$$

68 The $SU(3)_C$ symmetry component is the non-Abelian gauge group of quantum chromodynamics
69 (QCD), the theory of strong interactions. There are 8 generators for the $SU_C(3)$ group which
70 correspond to *gluons*, massless spin-1 gauge boson which carry the force of the strong interaction.

71 Gluon and quarks, the particles which interact with the strong force, carry a color charge C .

72 The $SU(2)_L \times U(1)_Y$ symmetry group represents the electroweak sector of the Standard Model.
73 There are 4 generators for this group, which correspond to the four massless gauge bosons W^1 , W^2 ,
74 W^3 , and B. From these massless gauge bosons are formed the massive mediators of the weak force,
75 the W^- , W^+ and Z^0 bosons, and the massless electromagnetic force carrier, the photon γ .

76 The interplay between the fermionic and bosonic fields that emerge from the G_{SM} symmetry
77 can be described through the Lagrangian in equation 1.2

$$\mathcal{L} = \mathcal{L}_{kin} + \mathcal{L}_\psi + \mathcal{L}_{Yuk} + \mathcal{L}_\phi \quad (1.2)$$

78 Each term in this Lagrangian describes a set of specific particle physics interactions. \mathcal{L}_{kin}
79 . with three families of quarks and leptons, and a scalar Higgs doublet. The standard model
80 has 12 gauge bosons: 8 gluons, 3 weak bosons, and the photon. [1]

81 The physics of the Standard Model of particle physics (SM) is summarized by the SM La-
82 grangian:

$$\mathcal{L}_{kin} = -\frac{1}{4}F_{\mu\nu}F^{\mu\nu} \quad (1.3)$$

83 Explain equation

84 Explain phenomonolyg

Chapter 2: The Large Hadron Collider

87 The Large Hadron Collider (LHC) is a 26.7km circular high-energy particle accelerator, span-
 88 ning the Swiss-French border near the city of Geneva, Switzerland [2]. The LHC occupies the
 89 tunnel constructed in 1989 for the Large Electron-Positron (LEP) Collider, and reaches a maxi-
 90 mum depth of 170m below the surface. The LHC is operated by the European Organization for
 91 Nuclear Research (CERN), the largest international scientific collaboration in the world.

93 The LHC accelerates protons and heavy ions and collides them at four interaction points around
 94 the ring, with a design center-of-mass energy per collision of $\sqrt{s} = 14$ TeV. Each interaction point
 95 is home to one of four detector experiments, which study the products of the collisions. The largest
 96 of these experiments is the ATLAS detector, a general purpose detector designed to study the Stan-
 97 dard Model and search for new physics that could be produced in LHC collisions [3]. The CMS
 98 detector is another general purpose detector, designed and operated independently of the ATLAS
 99 detector, but intended to probe the same range of physics [4]. The ALICE experiment is a dedi-
 100 cated heavy ion experiment, and the LHC-b experiment is a dedicated *b*-physics experiment [5] [6].

102 **2.1 LHC Timeline**

103 The first proton-proton collisions at the LHC were achieved in 2010 with a center-of-mass
 104 energy of $\sqrt{s} = 7$ TeV. Run 1 of the LHC took place between 2010 and 2013. The data collected
 105 during this time led to the discovery of the Higgs Boson in 2012 [7]. Between 2013 and 2015
 106 the LHC underwent the first Long Shutdown (LS1) during which time key upgrades to the physics
 107 detectors and the accelerator chain were installed. Run 2 of the LHC took place from 2015 to 2018



Figure 2.1: Timeline of LHC activities [9]

and achieved a center-of-mass energy of $\sqrt{s} = 13$ TeV. Between 2018 and 2022 the LHC underwent its second Long Shutdown (LS2). Run-3 of the LHC began in 2022 and achieved a center-of-mass energy of $\sqrt{s} = 13.6$ TeV. Run-3 is scheduled to continue through 2026, at which point the LHC machine and detectors will undergo upgrades for the *high luminosity* LHC (HL-LHC), which will increase the number of collisions by a factor of 5-10 with respect to the nominal LHC design [8].

2.2 Accelerator Physics

2.2.1 The Journey of a Proton

Protons which feed the LHC start as hydrogen gas. The electrons are removed from the hydrogen atoms through the use of strong electric fields. The linear accelerator (LINAC) then accelerates the H^- ions to an energy of 50 MeV. From here the H^- ions enter the Proton Synchrotron booster, where they are accelerated up to 1.4 GeV of energy. Subsequently they are sorted into bunches separated in time by 25 ns, where each bunch contains approximately 10^{11} protons. Next the bunches pass through the Proton Synchrotron (PS) and the Super Proton Synchrotron (SPS), where they reach energies of 25 GeV and 450 GeV respectively. Finally they are injected into the LHC as two

The CERN accelerator complex Complexe des accélérateurs du CERN

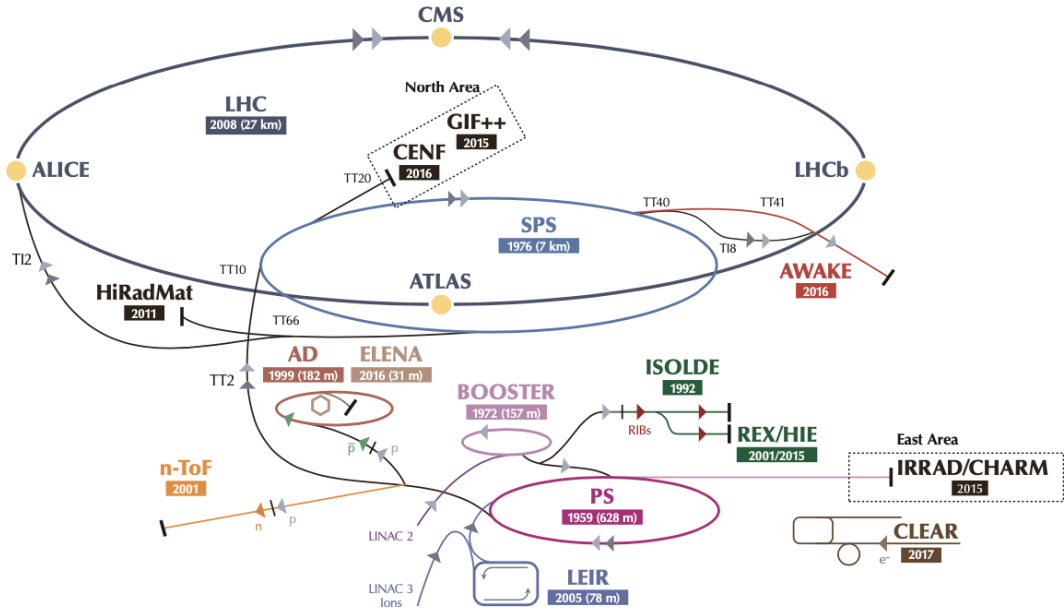


Figure 2.2: The LHC accelerator complex at CERN [11]

beams traveling in opposite direction. The original design allowed each beam to be accelerated up to 7 TeV of energy. Due to limitations with the magnet training, the highest energy actually achieved by the LHC beams during Run 2 was 6.5 TeV, giving a collision center-of-mass energy of $\sqrt{s} = 13$ TeV [10]. Figure 2.2 shows the full LHC accelerator complex.

127

Acceleration in the LHC is performed by eight radio frequency (RF) cavities located around the ring. Each RF cavity produces a 2MV electric field oscillating at 40 MHz. The 40MHz oscillation produces a point of stable equilibrium every 2.5ns. These points of equilibrium are synchronized with the occurrence of the proton bunches produced in the PS – a proton bunch occupies one out of every ten points of stable equilibrium, such that the bunches maintain a 25ns spacing [10].

133

134 2.2.2 Magnets

135 In addition to the acceleration cavities, the LHC houses 9593 superconducting magnets which
136 direct and focus the proton beam on its 27 kilometer journey. The magnets are comprised of super-
137 conducting Niobium-Titanium coils cooled to 1.9K by superfluid helium. As the beams approach
138 one of the four collision points around the ring, multipole magnets focus and squeeze the beam for
139 optimal collisions [10].

140 The LHC is divided into sections, where each section contains an a smoothly curving *arc* and
141 a straight *insertion*. The arcs are composed of 1232 large dipole magnets which bend the beam
142 to follow the roughly circular 27 km path. The main dipoles generate powerful 8.3 tesla magnetic
143 fields to achieve this bend. Each dipole magnet is 15 meters long and weighs 35 tonnes. The
144 dipoles work in conjunction with quadrupole magnets, which keep the particles in a focused beam,
145 and smaller sextupole, octupole and decapole magnets which tune the magnetic field at the ends of
146 the dipole magnets [12].

147 The straight insertion sections have different purposes depending on their location around the
148 ring: beam collisions, beam injection, beam dumping, or beam cleaning. At the four collision
149 points, insertion magnets squeeze the beam to ensure a highly focused collision. This is accom-
150 plished with a triplet of quadrupole magnets, which tighten the beam from 0.2 millimeters to just
151 16 micrometers in diameter. Insertion magnets also clean the beam, which prevents stray particles
152 from hitting sensitive components throughout the LHC. When the LHC is ready to dispose of a
153 beam of particles, beam dump magnets deflect the path of the beam into a straight line towards
154 a block of concrete and graphite that stops the beam. A dilution magnet then reduces the beam
155 intensity by a factor of 100,000 before the final stop [12]. Figure 2.3 shows the locations various
156 beam activities.

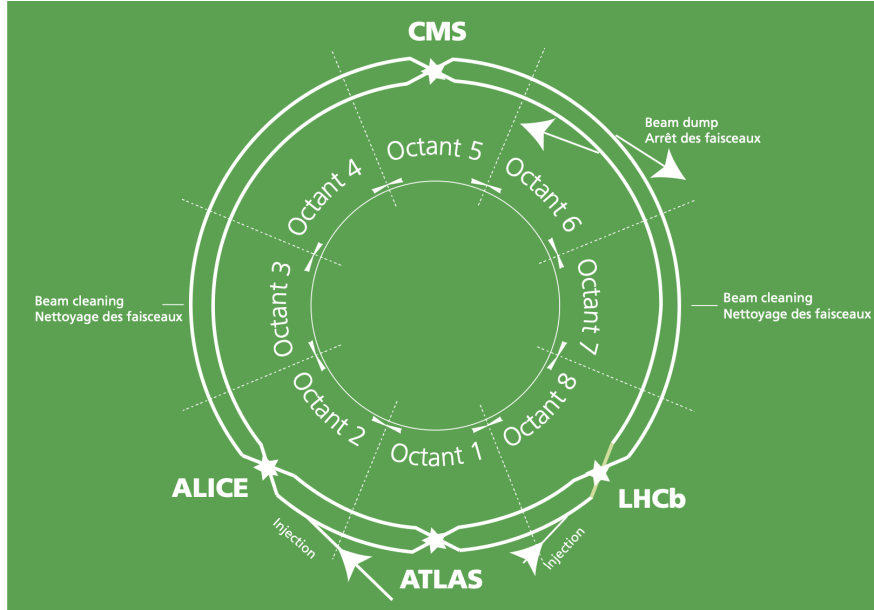


Figure 2.3: The octants of the LHC and location of various beam activities [10]

¹⁵⁷ 2.3 Luminosity

¹⁵⁸ Collisions at the LHC occur when the two beams of proton bunches cross at one of the four
¹⁵⁹ interaction points. The intensity of collisions is described by the instantaneous luminosity, the
¹⁶⁰ formula for which is given in equation 2.1.

$$L = \frac{f N_1 N_2}{4\pi \sigma_x \sigma_y} \quad (2.1)$$

¹⁶¹ Here f is the revolution frequency, N_1 and N_2 are the number of particle per bunch for each
¹⁶² beam, and σ_x , σ_y are the horizontal and vertical beam widths.

¹⁶³

¹⁶⁴ The instantaneous luminosity gives the number of the collisions that could be produced at the
¹⁶⁵ interaction point per cm^2 of cross-sectional area per second. The integrated luminosity is obtained
¹⁶⁶ by integrating the instantaneous luminosity over a given block of time, and measures the total num-
¹⁶⁷ ber of collisions which has occurred during that operation period. This is directly correlated with
¹⁶⁸ the size of the datasets collected by the LHC experiments.

169

170 The design peak luminosity of the LHC is $1.0 \times 10^{34} \text{ cm}^{-2}\text{s}^{-1}$. During Run 1 of the LHC the
171 peak instantaneous luminosity was $0.8 \times 10^{34} \text{ cm}^{-2}\text{s}^{-1}$. Over the course of Run 1 the LHC collected
172 a total integrated luminosity of 5.46 fb^{-1} at $\sqrt{s} = 7 \text{ TeV}$, and 22.8 fb^{-1} at $\sqrt{s} = 8 \text{ TeV}$. Following the
173 first long shutdown and upgrade phase of operations, the LHC achieved a center of mass energy
174 $\sqrt{s} = 13 \text{ TeV}$ at the beginning of Run 2 in 2015. The LHC was also able to deliver 2.0×10^{34}
175 $\text{cm}^{-2}\text{s}^{-1}$ peak instantaneous luminosity, double the design value. During LHC Run 2, from 2015-
176 2018, the LHC delivered 156 fb^{-1} of integrated luminosity for proton-proton collisions. Run 3 of
177 the LHC began in 2022, and is expected to deliver 250 fb^{-1} of integrated luminosity to the ATLAS
178 and CMS experiments by 2026 [9].

179

180 The goal of LHC physic analyses is to find and study rare events produced by interesting
181 physics processes. The cross section σ of a given process indicates the probability of that process
182 occurring given the beam conditions of the LHC. Multiplying the cross section by the integrated
183 luminosity of a dataset gives the expected number of events for that process within the dataset.

$$N_{\text{events}} = \int \sigma L(t) dt = \mathcal{L} \times \sigma \quad (2.2)$$

184 The cross section for most processes of interest, especially BSM processes, is several orders of
185 magnitude below the total cross section for the LHC. Therefore maximizing the number of events
186 produced in collisions is crucial to increase the likelihood of producing events from processes of
187 interest. For this reason, maximizing instantaneous luminosity is a key factor in accelerator design
188 and operation.

189

190

Chapter 3: The ATLAS Detector

191 The ATLAS detector is one of two general purpose physics detectors designed to study the
192 products of the proton-proton collisions produced by the LHC. The detectors is composed of a
193 variety of specialized subsystems, designed to fully capture the large array of physics processes
194 produced in the LHC. The apparatus is 25m high, 44m in length, and weighs over 7000 tons. Colli-
195 sions occur directly in the center of the apparatus, and the cylindrical design of the detector allows
196 a complete 360 view of any physics objects resulting from the collision to be reconstructed.

197

198 Two magnet systems provide strong magnetic fields, which bend the trajectory of charged
199 particles as they pass through the magnetic fields; this allows the calculation of the momentum
200 of the particles. A 2T solenoid magnet provides a uniform magnetic field to the inner layers of
201 the detector. Further out, a toroidal magnet system (TODO: how many toroids?) provides fields
202 strengths of 0.5 to 1T

203 **3.1 Coordinate System and Geometry**

204 The ATLAS detector employs a right hand cylindrical coordinate system. The z axis is aligned
205 with the beam line, and the x-y plane sits perpendicular to the beam line. The origin is centered on
206 the detector, such that the origin corresponds with the interaction point of the two colliding beams.
207 The detector geometry is usually characterized by polar coordinates, where the azimuthal angle ϕ
208 spans the x-y plane. The polar angle θ represents the angle away from the beam line, or z axis.
209 $\theta = 0$ aligns with the positive z -axis, and $\phi = 0$ aligns with the positive x-axis.

210

211 The polar coordinate θ is generally replaced by the Lorentz invariant quantity *rapidity* y .

$$y = \frac{1}{2} \ln\left(\frac{E + p_z}{E - p_z}\right) \quad (3.1)$$

212 This substitution is advantageous because objects in the detector are traveling at highly rela-
 213 tivistic speeds. The relativistic speed of objects passing through the ATLAS detector also means
 214 that the masses of the particles are generally small compared to their total energy. In the limit of
 215 zero mass, the rapidity y reduces to the *pseudorapidity* η , which can be calculated directly from
 216 the polar angle θ .

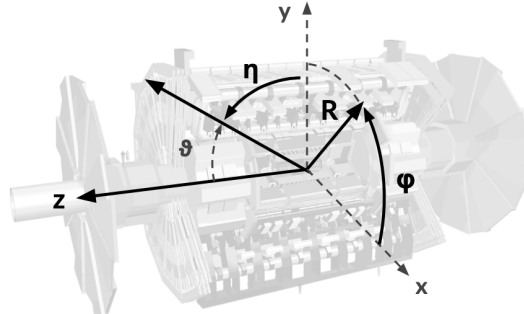
$$\eta = -\ln\left(\frac{\theta}{2}\right) \quad (3.2)$$

217 Figure 3.1a depicts the orientation of the coordinate system with respect to the ATLAS de-
 218 tector, while Figure 3.1b illustrates the relationship between θ , η , and the beamline axis z . The
 219 distance between physics objects in the detector is generally expressed in terms of the solid angle
 220 between them ΔR .

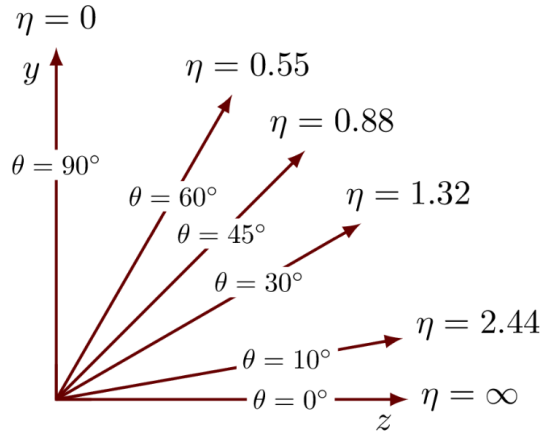
221

$$\Delta R = \sqrt{\Delta\phi^2 + \Delta\eta^2} \quad (3.3)$$

222 Head on proton-proton collisions are more likely to result in objects with a lot of energy in the
 223 transverse plane; glancing proton-proton collisions are more likely to result in objects where most
 224 of the energy is directed along the z -axis. Due to the importance of categorizing these objects,
 225 as well as the cylindrical design of the ATLAS detector, the detector is generally divided
 226 into regions in η . Each subsystem has a “central” or “barrel” region covering low $|\eta|$, while the
 227 “forward” or “endcap” regions cover $|\eta|$ up to 4.9. Each of the three main ATLAS subsystems will
 228 be discussed in the following sections.



(a) The ATLAS geometry



(b) Relationship between η and θ

Figure 3.1: ATLAS coordinate system and geometry

229 3.2 Inner Detector

230 The Inner Detector (ID) is the ATLAS subsystem closest to the interaction point. The primary
 231 purpose of the ID is to determine the charge, momentum, and trajectory of charged particles pass-
 232 ing through the detector. With this information the ID is also able to precisely determine interaction
 233 vertices.

234

235 The ID is composed of three sub-detectors; the pixel detector, the semiconductor tracker (SCT)
 236 and the transition radiation tracker (TRT). Figure ?? shows the location of these three subsystems
 237 with respect to each other and the interaction point.

238 3.2.1 Pixel Detector

239 The pixel detector is the first detector encountered by particles produced in LHC collisions.
 240 The original pixel detector consists of 3 barrel layers of silicon pixels, positioned at 4cm, 11cm
 241 and 14cm from the beamline. There are also 4 disks on each side positioned between 11 and 20cm,
 242 providing full coverage $|\eta| < 2.5$. The layers are comprised of silicon pixels each measuring 50
 243 μm by $300 \mu\text{m}$, with 140 million pixels in total. The pixels are organized into modules, which
 244 each contain a set of radiation hard readout electronics chips. In 2014, the Insertable B-layer

245 (IBL) was installed, creating a new innermost layer of the pixel detector sitting just 3.3cm from the
246 beamline. The pixels of the IBL measure $50\text{ }\mu\text{m}$ by $250\text{ }\mu\text{m}$, and cover a pseudo-rapidity range up
247 to $|\eta| < 3$. The IBL upgrade enhances the pixel detector's ability to reconstruct secondary vertices
248 associated with short-lived particles such as the b-quark. The improved vertex identification also
249 helped compensate for increasing pile-up in Run 2.

250 3.2.2 Semiconductor Tracker

251 The SCT provides at least 4 additional measurements of each charged particle. It employs
252 the same silicon technology as the Pixel Detector, but utilizes larger silicon strips which measure
253 $80\mu\text{m}$ by 12.4cm. The SCT is composed of 4 barrel layers, located between 30cm and 52cm from
254 the beamline, and 9 end-cap layers on each side. The SCT can distinguish tracks that are separated
255 by at least $200\mu\text{m}$.

256 3.2.3 Transition Radiation Tracker

257 The TRT provides an additional 36 hits per particle track. The detector relies on gas filled
258 straw tubes, a technology which is intrinsically radiation hard. The straws which are each 4mm in
259 diameter and up to 150cm in length and filled with xenon gas. The detector is composed of about
260 50000 barrel region straws and 640000 end-cap straws, comprising 420000 electronic readout
261 channels. Each channel provides a drift time measurement with a spatial resolution of $170\mu\text{m}$
262 per straw. As charged particles pass through the detector and interact with the xenon, transition
263 radiation is emitted. The use of two different drift time thresholds allows the detector to distinguish
264 between tracking hits and transition radiation hits.

265 3.3 Calorimeters

266 The ATLAS calorimeter system is responsible for measuring the energy of electromagnetically
267 and hadronically interacting particles passing through the detector. The calorimeters are located
268 just outside the central solenoid magnet, which encloses the inner detectors. The calorimeters also

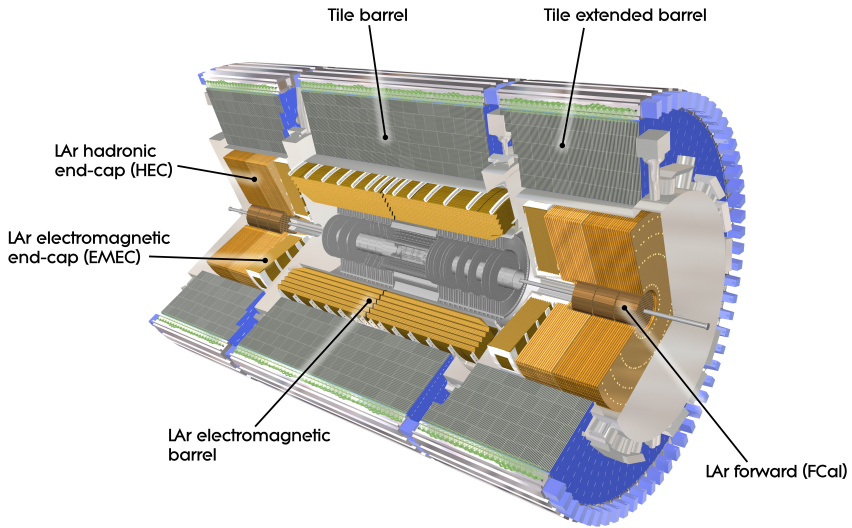


Figure 3.2: ATLAS calorimetry system [13]

269 stop most known particles, which the exception of muons and neutrinos, preventing them from
 270 traveling to the outermost layers of the detector. The ATLAS calorimetry system is composed of
 271 two subsystems - the Liquid Argon (LAr) calorimeter for electromagnetic calorimetry and the Tile
 272 calorimeter for hadronic calorimetry. The full calorimetry system is shown in figure 3.2.

273 3.3.1 Liquid Argon Calorimeter

274 The LAr calorimeter is a sampling calorimeter designed to trigger on and measure the energies
 275 of electromagnetic particles, as well as hadronic particles in the high η regions. It is divided in sev-
 276 eral regions, as shown in Figure 3.2. For the region $|\eta| < 1.4$, the electromagnetic barrel (EMB) is
 277 responsible for electronic calorimetry, and provides high resolution energy, timing, and position
 278 measurements for electrons and photons passing through the detector. The electromagnetic endcap
 279 (EMEC) provides additional EM calorimetry up to $|\eta| < 3.2$. In the region $1.4 < |\eta| < 3.2$, the
 280 hadronic endcap (HEC) provides hadronic calorimetry. For hadronic calorimetry In the region
 281 $|\eta| < 1.4$, corresponding to a detector radii $> 2.2\text{m}$, the less expensive tile calorimeter (discussed
 282 in the next section) is used instead. A forward calorimeter (FCAL) extends the hadronic calorime-
 283 try coverage up to $3.1 < |\eta| = 4.8$ [14].

284

285 The LAr calorimeter is composed of liquid argon sandwiched between layers of absorber mate-
286 rial and electrodes. Liquid argon is advantageous as a calorimeter active medium due to its natural
287 abundance and low cost, chemical stability, radiation tolerance, and linear response over a large
288 energy range [15]. The calorimeter is cooled to 87k by three cryostats: one barrel cryostat encom-
289 passing the EMB, and two endcap cryostats. The barrel cryostat also encloses the solenoid which
290 produces the 2T magnetic field for the inner detector. Front end electronics are housed outside the
291 cryostats and are used to process, store and transfer the calorimeter signals.

292

293 **Electromagnetic Calorimeter**

294 For the electromagnetic calorimeters, the layers of electrodes and absorber materials are ar-
295 ranged in an an accordion shape, as illustrated in Figure 3.3. The accordion shape ensures that
296 each half barrel is continuous in the azimuthal angle, which is a key feature for ensuring consistent
297 high resolution measurements. Liquid argon permeates the space between the lead absorber plates,
298 and a multilayer copper-polymide readout board runs through the center of the liquid argon filled
299 gap.

300

301 The detection principle for the LAr calorimeter is the current created by electrons which are
302 released when a charged particle ionizes the liquid argon. In the barrel region, the electrons are
303 driven towards the center electrodes by a 2000V potential with a drift time of less than 450ns [16].
304 In the endcaps the voltage varies as a function of the radius in order to maintain a flat response [14].
305 The amount of current produced by the ionized electrons is proportional to the energy of the parti-
306 cle creating the signal. Figure ?? shows the shape of the signal produced in the LAr calorimeter,
307 before and after it undergoes shaping during the readout process. The shaping of the pulse enforces
308 a positive peak and a negative tail, which ensures that subsequence pulses can be separated with
309 the precision required for the 25ns LHC bunch spacing [14].

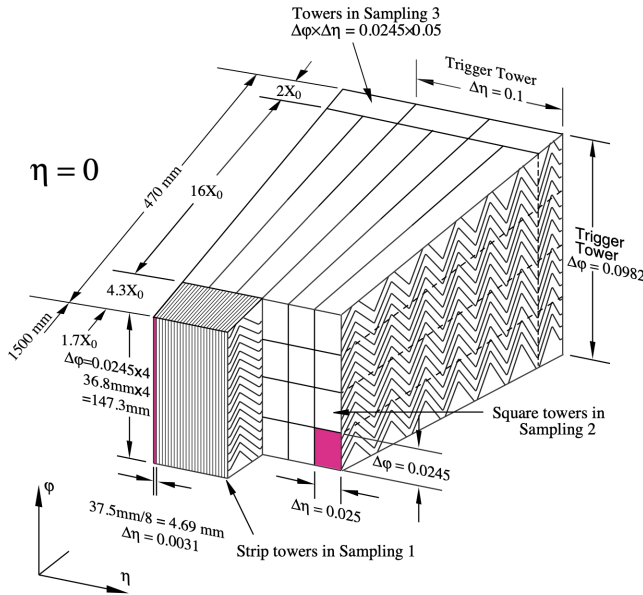


Figure 3.3: Diagram of a segment of the EMB, demonstrating the accordion plate arrangement [14]

310

311 **Hadronic End-cap Calorimeter**

312 The HEC sits radially beyond the EMEC. The copper absorber plates in the HEC are oriented
 313 perpendicular to the beamline, with LAr as the active medium. Each end-cap is divided into two
 314 independent wheels; the inner wheel uses 25mm copper plates, while the outer wheel uses 50mm
 315 plates as a cost saving measure. In each wheel, the 8.5mm plate gap is crossed by three parallel
 316 electrodes, creating an effective drift distance of 1.8mm. This gap is illustrated in Figure 3.5.
 317 Each wheel is divided into 32 wedge-shaped modules, each containing their own set of readout
 318 electronics.

319 **Forward Calorimeter**

320 The forward range is covered by the FCAL, which provides both electromagnetic and hadronic
 321 calorimetry. It is composed of three active cylindrical modules; one EM module with copper

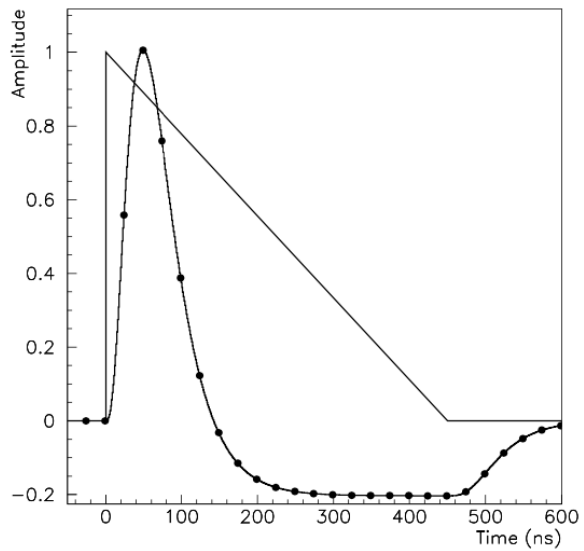


Figure 3.4: A LAr pulse as produced in the detector (triangle) and after shaping (curve) [14]

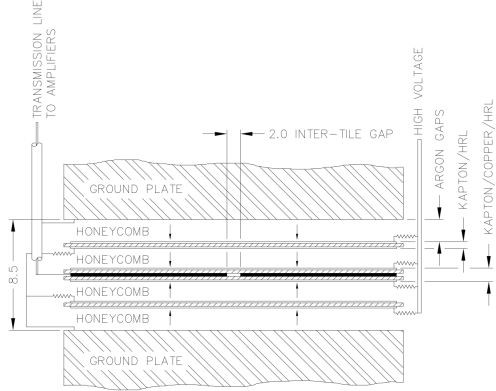


Figure 3.5: Readout gap structure in HEC [14]

322 absorber plates, and two hadronic modules with tungsten absorber plates. The plates are oriented
323 perpendicular to the beamline, and LAr is used as the active material throughout.

324 3.3.2 Tile Calorimeter

325 The tile calorimeter (TileCal) provides hadronic calorimetry in the region $\eta < 1.7$, and sur-
326 rounds the LAr calorimeter. It is responsible for measurements of jet energy and jet substructure,
327 and also plays an important role in electron isolation and triggering (including muons) [17]. Tile-
328 Cal is composed of 3 sections, as shown in figure 3.2; a barrel calorimeter sits directly outside the
329 LAr EMB and provides coverage up to $\eta < 1.0$. Two extended barrel sections sit outside the LAr
330 endcaps and cover the region $0.8 < \eta < 1.7$.

331

332 TileCal is a sampling calorimeter composed of steel and plastic scintillator plates as illustrated
333 in Figure 3.6. A total of 460,000 scintillators are read out by wavelength-shifting fibers. The
334 fibers are gathered to define cells and in turn read out by photomultiplier tubes, which amplify
335 the signal and convert it to an electrical signature. Each cell has an approximate granularity of
336 $\Delta\eta \times \Delta\phi = 0.1 \times 0.1$. Each barrel is divided azimuthally into 64 independent modules, an example
337 of which is show in Figure 3.6. The modules are each serviced by front-end electronic housed in a
338 water-cooled drawer on the exterior of the module.

339

340 The detection principle of the TileCal is the production of light from hadronic particles inter-
341 acting with the scintillating tiles. When a hadronic particle hits the steel plate, a shower of particles
342 are produced. The interaction of the shower with the plastic scintillator produces photons, the num-
343 ber and intensity of which are proportional to the original particle's energy.

344

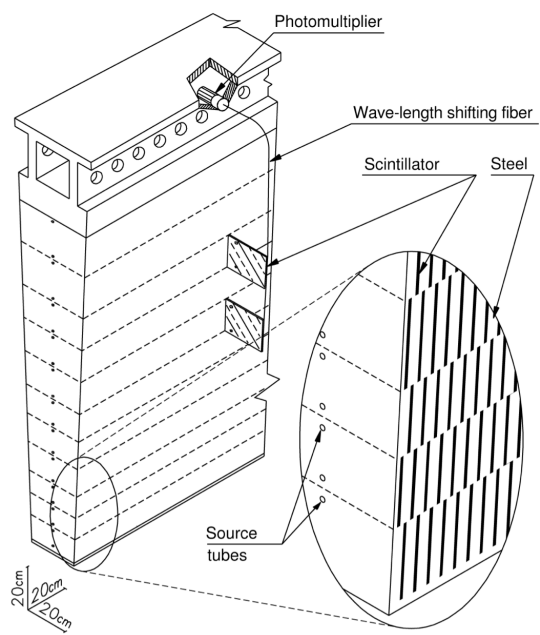


Figure 3.6: TileCal wedge module [17]

Conclusion or Epilogue

346 Use this page for your epilogue or conclusion if applicable; please use only one of the titles
347 for this page. Otherwise, you may delete it. Use this page for your epilogue or conclusion if
348 applicable; please use only one of the titles for this page. Otherwise, you may delete it. Use this
349 page for your epilogue or conclusion if applicable; please use only one of the titles for this page.
350 Otherwise, you may delete it. Use this page for your epilogue or conclusion if applicable; please
351 use only one of the titles for this page. Otherwise, you may delete it. Use this page for your
352 epilogue or conclusion if applicable; please use only one of the titles for this page. Otherwise,
353 you may delete it. Use this page for your epilogue or conclusion if applicable; please use only one
354 of the titles for this page. Otherwise, you may delete it. Use this page for your epilogue or
355 conclusion if applicable; please use only one of the titles for this page. Otherwise, you may delete
356 it. Use this page for your epilogue or conclusion if applicable; please use only one of the titles for
357 this page. Otherwise, you may delete it. Use this page for your epilogue or conclusion if
358 applicable; please use only one of the titles for this page. Otherwise, you may delete it. Use this
359 page for your epilogue or conclusion if applicable; please use only one of the titles for this page.
360 Otherwise, you may delete it. Use this page for your epilogue or conclusion if applicable; please
361 use only one of the titles for this page. Otherwise, you may delete it. Use this page for your
362 epilogue or conclusion if applicable; please use only one of the titles for this page. Otherwise,
363 you may delete it. Use this page for your epilogue or conclusion if applicable; please use only one
364 of the titles for this page. Otherwise, you may delete it. Use this page for your epilogue or
365 conclusion if applicable; please use only one of the titles for this page. Otherwise, you may delete

366 it. Use this page for your epilogue or conclusion if applicable; please use only one of the titles for
367 this page. Otherwise, you may delete it. Use this page for your epilogue or conclusion if
368 applicable; please use only one of the titles for this page. Otherwise, you may delete it. Use this
369 page for your epilogue or conclusion if applicable; please use only one of the titles for this page.
370 Otherwise, you may delete it. Use this page for your epilogue or conclusion if applicable; please
371 use only one of the titles for this page. Otherwise, you may delete it. Use this page for your
372 epilogue or conclusion if applicable; please use only one of the titles for this page. Otherwise,
373 you may delete it. Use this page for your epilogue or conclusion if applicable; please use only one
374 of the titles for this page. Otherwise, you may delete it. Use this page for your epilogue or
375 conclusion if applicable; please use only one of the titles for this page. Otherwise, you may delete
376 it. Use this page for your epilogue or conclusion if applicable; please use only one of the titles for
377 this page. Otherwise, you may delete it. Use this page for your epilogue or conclusion if
378 applicable; please use only one of the titles for this page. Otherwise, you may delete it. Use this
379 page for your epilogue or conclusion if applicable; please use only one of the titles for this page.
380 Otherwise, you may delete it. Use this page for your epilogue or conclusion if applicable; please
381 use only one of the titles for this page. Otherwise, you may delete it. Use this page for your
382 epilogue or conclusion if applicable; please use only one of the titles for this page. Otherwise,
383 you may delete it. Use this page for your epilogue or conclusion if applicable; please use only one
384 of the titles for this page. Otherwise, you may delete it. Use this page for your epilogue or
385 conclusion if applicable; please use only one of the titles for this page. Otherwise, you may delete
386 it. Use this page for your epilogue or conclusion if applicable; please use only one of the titles for
387 this page. Otherwise, you may delete it. Use this page for your epilogue or conclusion if
388 applicable; please use only one of the titles for this page. Otherwise, you may delete it. Use this
389 page for your epilogue or conclusion if applicable; please use only one of the titles for this page.
390 Otherwise, you may delete it. Use this page for your epilogue or conclusion if applicable; please
391 use only one of the titles for this page. Otherwise, you may delete it. Use this page for your
392 epilogue or conclusion if applicable; please use only one of the titles for this page. Otherwise,

393 you may delete it. Use this page for your epilogue or conclusion if applicable; please use only one
394 of the titles for this page. Otherwise, you may delete it. Use this page for your epilogue or
395 conclusion if applicable; please use only one of the titles for this page. Otherwise, you may delete
396 it. Use this page for your epilogue or conclusion if applicable; please use only one of the titles for
397 this page. Otherwise, you may delete it. Use this page for your epilogue or conclusion if
398 applicable; please use only one of the titles for this page. Otherwise, you may delete it. Use this
399 page for your epilogue or conclusion if applicable; please use only one of the titles for this page.
400 Otherwise, you may delete it. Use this page for your epilogue or conclusion if applicable; please
401 use only one of the titles for this page. Otherwise, you may delete it. Use this page for your
402 epilogue or conclusion if applicable; please use only one of the titles for this page. Otherwise,
403 you may delete it. Use this page for your epilogue or conclusion if applicable; please use only one
404 of the titles for this page. Otherwise, you may delete it. Use this page for your epilogue or
405 conclusion if applicable; please use only one of the titles for this page. Otherwise, you may delete
406 it. Use this page for your epilogue or conclusion if applicable; please use only one of the titles for
407 this page. Otherwise, you may delete it. Use this page for your epilogue or conclusion if
408 applicable; please use only one of the titles for this page. Otherwise, you may delete it. Use this
409 page for your epilogue or conclusion if applicable; please use only one of the titles for this page.
410 Otherwise, you may delete it. Use this page for your epilogue or conclusion if applicable; please
411 use only one of the titles for this page. Otherwise, you may delete it. Use this page for your
412 epilogue or conclusion if applicable; please use only one of the titles for this page. Otherwise,
413 you may delete it. Use this page for your epilogue or conclusion if applicable; please use only one
414 of the titles for this page. Otherwise, you may delete it. Use this page for your epilogue or
415 conclusion if applicable; please use only one of the titles for this page. Otherwise, you may delete
416 it. Use this page for your epilogue or conclusion if applicable; please use only one of the titles for
417 this page. Otherwise, you may delete it. Use this page for your epilogue or conclusion if
418 applicable; please use only one of the titles for this page. Otherwise, you may delete it. Use this
419 page for your epilogue or conclusion if applicable; please use only one of the titles for this page.

420 Otherwise, you may delete it. Use this page for your epilogue or conclusion if applicable; please
421 use only one of the titles for this page. Otherwise, you may delete it. Use this page for your
422 epilogue or conclusion if applicable; please use only one of the titles for this page. Otherwise,
423 you may delete it. Use this page for your epilogue or conclusion if applicable; please use only one
424 of the titles for this page. Otherwise, you may delete it. Use this page for your epilogue or
425 conclusion if applicable; please use only one of the titles for this page. Otherwise, you may delete
426 it. Use this page for your epilogue or conclusion if applicable; please use only one of the titles for
427 this page. Otherwise, you may delete it. Use this page for your epilogue or conclusion if
428 applicable; please use only one of the titles for this page. Otherwise, you may delete it. Use this
429 page for your epilogue or conclusion if applicable; please use only one of the titles for this page.
430 Otherwise, you may delete it. Use this page for your epilogue or conclusion if applicable; please
431 use only one of the titles for this page. Otherwise, you may delete it. Use this page for your
432 epilogue or conclusion if applicable; please use only one of the titles for this page. Otherwise,
433 you may delete it. Use this page for your epilogue or conclusion if applicable; please use only one
434 of the titles for this page. Otherwise, you may delete it. Use this page for your epilogue or
435 conclusion if applicable; please use only one of the titles for this page. Otherwise, you may delete
436 it. Use this page for your epilogue or conclusion if applicable; please use only one of the titles for
437 this page. Otherwise, you may delete it. Use this page for your epilogue or conclusion if
438 applicable; please use only one of the titles for this page. Otherwise, you may delete it. Use this
439 page for your epilogue or conclusion if applicable; please use only one of the titles for this page.
440 Otherwise, you may delete it. Use this page for your epilogue or conclusion if applicable; please
441 use only one of the titles for this page. Otherwise, you may delete it. Use this page for your
442 epilogue or conclusion if applicable; please use only one of the titles for this page. Otherwise,
443 you may delete it. Use this page for your epilogue or conclusion if applicable; please use only one
444 of the titles for this page. Otherwise, you may delete it. Use this page for your epilogue or
445 conclusion if applicable; please use only one of the titles for this page. Otherwise, you may delete
446 it.

References

- [1] M. Tanabashi et al. “Review of Particle Physics”. In: *Phys. Rev. D* 98 (3 2018), pp. 847–851.
- [2] Lyndon Evans and Philip Bryant. “LHC Machine”. In: *Journal of Instrumentation* 3.08 (2008), S08001.
- [3] “The ATLAS Experiment at the CERN Large Hadron Collider”. In: *JINST* 3 (2008). Also published by CERN Geneva in 2010, S08003.
- [4] “The CMS experiment at the CERN LHC”. In: *Journal of Instrumentation* 3.08 (2008), S08004.
- [5] “The ALICE experiment at the CERN LHC”. In: *Journal of Instrumentation* 3.08 (2008), S08002.
- [6] “The LHCb Detector at the LHC”. In: *Journal of Instrumentation* 3.08 (2008), S08005.
- [7] Aad G., et al. (ATLAS Collaboration and CMS Collaboration). “Combined Measurement of the Higgs Boson Mass in pp Collisions at $\sqrt(s) = 7$ and 8 TeV with the ATLAS and CMS Experiments”. In: *Phys. Rev. Lett.* 114 (19 2015), p. 191803.
- [8] O. Aberle et al. *High-Luminosity Large Hadron Collider (HL-LHC): Technical design report*. CERN Yellow Reports: Monographs. Geneva: CERN, 2020.
- [9] *The High-Luminosity LHC*. <https://voisins.web.cern.ch/high-luminosity-lhc-hl-lhc>. Accessed: 2024-01-05.
- [10] Ana Lopes and Melissa Loyse Perrey. *FAQ-LHC The guide*. 2022.
- [11] Esma Mobs. “The CERN accelerator complex in 2019. Complexe des accélérateurs du CERN en 2019”. In: (2019). General Photo.
- [12] *Pulling together: Super Conducting electromagnets*. <https://home.cern/science/engineering/pulling-together-superconducting-electromagnets>. Accessed: 2024-01-05.
- [13] Joao Pequenao. *Computer Generated image of the ATLAS calorimeter*. 2008.
- [14] *ATLAS liquid-argon calorimeter: Technical Design Report*. Technical design report. ATLAS. Geneva: CERN, 1996.

- ⁴⁷⁴ [15] H A Gordon. “Liquid argon calorimetry for the SSC”. In: ().
- ⁴⁷⁵ [16] Henric Wilkens and (on behalf ofthe ATLAS LArg Collaboration). “The ATLAS Liquid
⁴⁷⁶ Argon calorimeter: An overview”. In: *Journal of Physics: Conference Series* 160.1 (2009),
⁴⁷⁷ p. 012043.
- ⁴⁷⁸ [17] *Technical Design Report for the Phase-II Upgrade of the ATLAS Tile Calorimeter*. Tech.
⁴⁷⁹ rep. Geneva: CERN, 2017.

Appendix A: Experimental Equipment

482 Lorem ipsum dolor sit amet, consectetur adipiscing elit, sed do eiusmod tempor incididunt ut
483 labore et dolore magna aliqua. Ut enim ad minim veniam, quis nostrud exercitation ullamco laboris
484 nisi ut aliquip ex ea commodo consequat. Duis aute irure dolor in reprehenderit in voluptate velit
485 esse cillum dolore eu fugiat nulla pariatur. Excepteur sint occaecat cupidatat non proident, sunt in
486 culpa qui officia deserunt mollit anim id est laborum.

487

488

Appendix B: Data Processing

489 Lorem ipsum dolor sit amet, consectetur adipiscing elit, sed do eiusmod tempor incididunt ut
490 labore et dolore magna aliqua. Ut enim ad minim veniam, quis nostrud exercitation ullamco laboris
491 nisi ut aliquip ex ea commodo consequat. Duis aute irure dolor in reprehenderit in voluptate velit
492 esse cillum dolore eu fugiat nulla pariatur. Excepteur sint occaecat cupidatat non proident, sunt in
493 culpa qui officia deserunt mollit anim id est laborum.